Vesicle dynamics in shear and capillary flows

2005 J. Phys.: Condens. Matter 17 S3439

(http://iopscience.iop.org/0953-8984/17/45/032)

INSTITUTE OF PHYSICS PUBLISHING JOURNAL OF PHYSICS: CONDENSED MATTER

J. Phys.: Condens. Matter **17** (2005) S3439–S3444 doi:10.1088/0953-8984/17/45/032

Vesicle dynamics in shear and capillary flows

Hiroshi Noguchi and Gerhard Gompper

Institut für Forstköperforschung, Forschungszentrum Jülich 52425 Jülich, Germany

E-mail: hi.noguchi@fz-juelich.de

Received 16 September 2005
Published 28 October 2005
Online at stacks.iop.org/JPhysCM/17/S3439

Abstract

The deformation of vesicles in flow is studied by a mesoscopic simulation technique, which combines multi-particle collision dynamics for the solvent with a dynamically triangulated surface model for the membrane. Shape transitions are investigated both in simple shear flows and in cylindrical capillary flows. We focus on reduced volumes, where the discocyte shape of fluid vesicles is stable, and the prolate shape is metastable. In simple shear flow at low membrane viscosity, the shear induces a transformation from discocyte to prolate with increasing shear rate, while at high membrane viscosity, the shear induces a transformation from prolate to discocyte, or tumbling motion accompanied by oscillations between these two morphologies. In capillary flow, at small flow velocities the symmetry axis of the discocyte is found not to be oriented *perpendicular* to the cylinder axis. With increasing flow velocity, a transition to a prolate shape occurs for fluid vesicles, while vesicles with shear-elastic membranes (like red blood cells) transform into a coaxial parachute-like shape.

1. Introduction

Vesicles are closed lipid-bilayer membranes of usually spherical topology. They show a rich variety of morphologies depending on the lipid architecture and their environment. In thermal equilibrium, vesicle shapes have been investigated intensively using a curvature-elastic model and are now understood very well [1]. By comparison, the behaviour of vesicles in flow fields is much less explored.

The dynamical behaviour of vesicles in flow is an important subject not only of fundamental research but also in medical applications. For example, in microvessels or glass capillaries, the apparent viscosity of blood depends on the tube diameter (Fåhraeus–Lindqvist effect) [2, 3]. In diseases such as diabetes mellitus, red blood cells (RBCs) have reduced deformability, which leads to an increase of the apparent blood viscosity [4].

The shapes of lipid vesicles and RBCs are determined by the competition of the mechanical properties of the membrane, the constraints of constant volume V and constant surface area S, and the external hydrodynamic forces. The properties of the membrane of fluid vesicles are

determined by its curvature elasticity and two-dimensional viscosity $\eta_{\rm mb}$. The cytoskeleton of RBCs, which consists of a triangular spectrin network attached at some anchoring points to the lipid bilayer, induces a shear elasticity of the compound membrane. The cytoplasm of RBCs behaves as a Newtonian fluid.

In simple shear flow, two types of vesicle dynamics are well known, a steady state with a *tank-treading motion* of the membrane and a finite inclination angle with the flow direction, and an unsteady state with a *tumbling motion* [5]. On the other hand, RBCs are known to form *parachute shapes* in microvessels and glass capillaries [2, 4]. Recently, we have studied shape transitions in the both flows using a three-dimensional mesoscopic simulation technique [6–8]. In this paper, we briefly review the simulation method and some of the key results, and compare the dynamical behaviours in simple shear flow and in capillary flow.

2. Methods

We employ a mesoscopic approach, which combines a particle-based hydrodynamics model [9–11] for the solvent and a coarse-grained, dynamically triangulated surface model [12, 13] for the membrane.

The mesoscale hydrodynamics method is known under the name of multi-particle collision dynamics (MPCD) or stochastic rotation dynamics (SRD). We briefly explain here the simulation technique; details of methods for simple shear and capillary flows are described in [7] and [8], respectively. The solvent is described by $N_{\rm s}$ point-like particles of mass $m_{\rm s}$. The algorithm of MPCD consists of alternating streaming and collision steps. In the streaming step, the particles move ballistically. In the collision step, the particles are sorted into cubic boxes of lattice constant a. The collision step consists of a stochastic rotation of the relative velocities of each particle in a box around an axis, which is chosen with random orientation for each box.

The fluid membrane is described by $N_{\rm mb}$ vertices which are connected by tethers to form a triangular network. The vertices have excluded volume and mass $m_{\rm mb}$. Soft pairwise potentials are employed for the tether-bond and excluded volume interactions [7]. The average bond length is chosen to equal the lattice constant a of the collision boxes. The shapes and fluctuations of the membrane are controlled by curvature elasticity with the energy $H_{\rm cv} = (\kappa/2)\int (C_1 + C_2)^2\,{\rm d}S$, where κ is the bending rigidity, and C_1 and C_2 are the principal curvatures at each point of the membrane. To model the fluidity of the membrane, bonds can be flipped between the two possible diagonals of two adjacent triangles. The membrane viscosity $\eta_{\rm mb}$ is varied by the bond-flip rate. The volume V and surface area S of a vesicle are kept constant to about 1% accuracy by the constraint potentials. The RBC membrane is modelled as a composite network, which consists of a dynamically triangulated surface as in the case of fluid vesicles, coupled to an additional network of harmonic springs with fixed connectivity (no bond-flip). The same number of the bonds is used for both the fluid and the tethered networks. We denote this model as an 'elastic vesicle'. The results presented in this paper are obtained for bending rigidity $\kappa = 20k_{\rm B}T$ and shear modulus $\mu = 110k_{\rm B}T/R_0^2$ (so $\mu R_0^2/\kappa = 5.5$).

To induce a shear flow, we employ Lees–Edwards boundary conditions, which give a linear flow profile $(v_x, v_y, v_z) = (\dot\gamma z, 0, 0)$ in the MPCD fluid. We use cylindrical capillaries with radius $R_{\rm cap} = 8a$ for capillary flows. Periodic boundary conditions are used in the flow (z) direction. A gravitation force is used to generate flow. The solvent interacts with the membrane and the capillary wall with no-slip boundary conditions [7, 10].

In this paper, we focus on vesicles with the reduced volume $V^* = V/(4\pi R_0^3/3) = 0.59$, where $R_0 = \sqrt{S/4\pi} = 5.7a$ is the effective vesicle radius. At this reduced volume, a biconcave

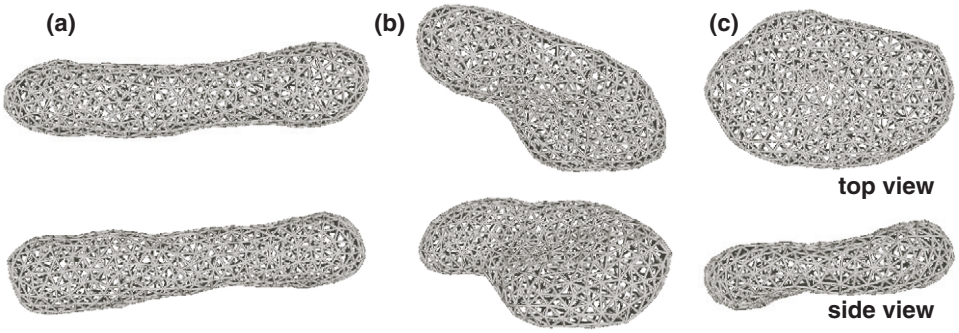

Figure 1. Sequential snapshots of the fluid vesicle in shear flow; compare figure 2(a). (a) $t/\tau = 5.4$ (prolate shape). (b) $t/\tau = 35.3$ (transient shape). (c) $t/\tau = 57.1$ (discoidal shape).

discocyte is the equilibrium shape, and a prolate ellipsoid and a stomatocyte are metastable in the absence of flow [1, 6]. The fluids in the interior and exterior of the vesicle are taken to be the same, in particular to have the same viscosity η_0. The results are conveniently expressed in terms of dimensionless variables: the reduced shear rate $\dot{\gamma}^* = \dot{\gamma}\tau$, where $\tau = \eta_0 R_0^3/\kappa$ is the longest relaxation time of the vesicle, and the relative membrane viscosity $\eta^*_{\rm mb} = \eta_{\rm mb}/\eta_0 R_0$. The membrane viscosity is varied in simple shear flows, and kept constant at $\eta_{\rm mb}/\eta_0 R_0 = 3$ in capillary flows.

3. Results and discussion

3.1. Simple shear flow

For membrane viscosity $\eta^*_{\rm mb} = 0$, both discoidal and prolate vesicles exhibit tank-treading motion at all investigated shear rates. For shear rates $\dot{\gamma}^* \gtrsim 1.4$, the discocyte vesicle transforms into a prolate, while the vesicle retains its shape for smaller shear rates. This shape transformation can be understood from the decomposition of the simple shear flow as a linear combination of a rotational flow and a elongational flow (where the elongational direction forms a 45° angle with the flow direction). The rotational component drives the tank-treading membrane rotation. The elongational component provides a force to overcome the free-energy barrier between discocyte and prolate shapes at higher shear rates.

With increasing membrane viscosity $\eta^*_{\rm mb}$, the inclination angle θ decreases, until a transition from tank-treading to tumbling motion occurs at small positive θ. The qualitative features of the simulation data are reproduced by the theory of Keller and Skalak (KS) [5] for fluid droplets of fixed, ellipsoidal shape in shear flow.

The inclination angle θ of prolates decreases faster than that of discocytes with increasing $\eta^*_{\rm mb}$. At a large membrane viscosity of $\eta^*_{\rm mb} = 1.62$, the prolate enters the tumbling phase, while the discocyte remains in the tank-treading phase. Remarkably, for small shear rates, the (metastable) prolate starts tumbling, but after a π or 2π rotation, transforms into a tank-treading discocyte. This transformation is illustrated by a few snapshots in figure 1. The time dependence of the asphericity α and the inclination angle θ are shown in figure 2(a). Here, the asphericity $\alpha = (1/2)[(\lambda_1 - \lambda_2)^2 + (\lambda_2 - \lambda_3)^2 + (\lambda_3 - \lambda_1)^2]/(\lambda_1 + \lambda_2 + \lambda_3)^2$, with the eigenvalues $\lambda_1, \lambda_2, \lambda_3$ of the moment-of-inertia tensor, is a convenient measure to distinguish oblate and prolate shapes, with $\alpha \simeq 0.2$ for the discocyte and $\alpha \simeq 0.8$ for the prolate shape (at $V^* = 0.59$). For larger shear rates, the discocyte transforms into a prolate,

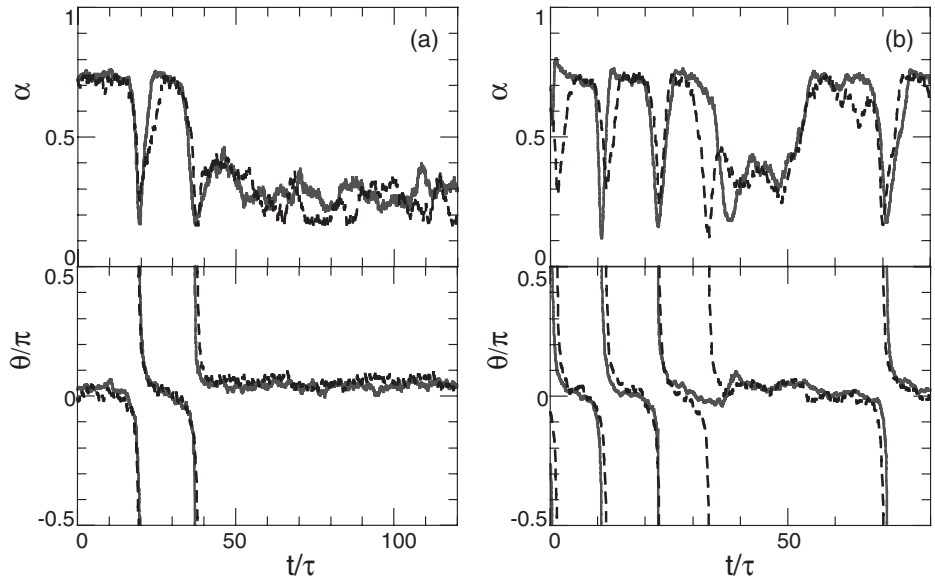

Figure 2. Time dependence of asphericity α and inclination angle θ, for (a) $\dot{\gamma}^* = 1.84$ and (b) $\dot{\gamma}^* = 2.76$, at $\eta^*_{\rm mb} = 1.62$ and $V^* = 0.59$. The broken lines are obtained from equations (1) and (2) with $\zeta_\alpha = 100$, $A = 12$, and $B(\alpha) = 1.1 - 0.17\alpha$.

but the tumbling motion continues, accompanied by shape oscillations between prolate and discocyte; see figure 2(b). Thus, four phases are obtained.

(i) At small $\dot{\gamma}^*$ and small $\eta^*_{\rm mb}$, both discocyte and prolate vesicles show steady tank-treading motion.
(ii) At large $\dot{\gamma}^*$ and small $\eta^*_{\rm mb}$, the discocyte transits to a tank-treading prolate.
(iii) At small $\dot{\gamma}^*$ and large $\eta^*_{\rm mb}$, a tumbling prolate transits to a tank-treading discocyte.
(iv) At large $\dot{\gamma}^*$ and large $\eta^*_{\rm mb}$, tumbling motion occurs with shape oscillations between prolate and discocyte.

The threshold for the discocyte-to-prolate transition increases from $\dot{\gamma}^* = 1.4$ to 2.0 with an increase in $\eta^*_{\rm mb}$ from 0 to 1.6.

We propose a simple stochastic phenomenological model [7] to describe the vesicle dynamics including morphological changes,

$$\zeta_\alpha \dot{\alpha} = -\kappa^{-1} \partial F/\partial\alpha + A\dot{\gamma}^* \sin(2\theta) + \zeta_\alpha g_\alpha(t) \tag{1}$$

$$\dot{\theta} = \tfrac{1}{2}\dot{\gamma}^*\{-1 + B(\alpha)\cos(2\theta)\} + g_\theta(t), \tag{2}$$

where $g_\alpha(t)$ and $g_\theta(t)$ are Gaussian white noises, which obey the fluctuation-dissipation theorem. The first and second terms of equation (1) are the forces due to curvature elasticity and shear flow, respectively. The thermodynamic force $\partial F/\partial\alpha$ is determined by the free energy $F(\alpha)$. Equation (2) is adopted from KS theory [5], where the coefficient B now depends on the (time-dependent) asphericity α. For $B > 1$, a steady angle $\theta = 0.5 \arccos(1/B)$ exists and tank-treading motion occurs, while for $B < 1$, there is no stable angle and tumbling motion occurs. This simple model reproduces the vesicle dynamics very well, both for the prolate-to-discocyte transformation in figure 2(a) and the shape oscillations in figure 2(b).

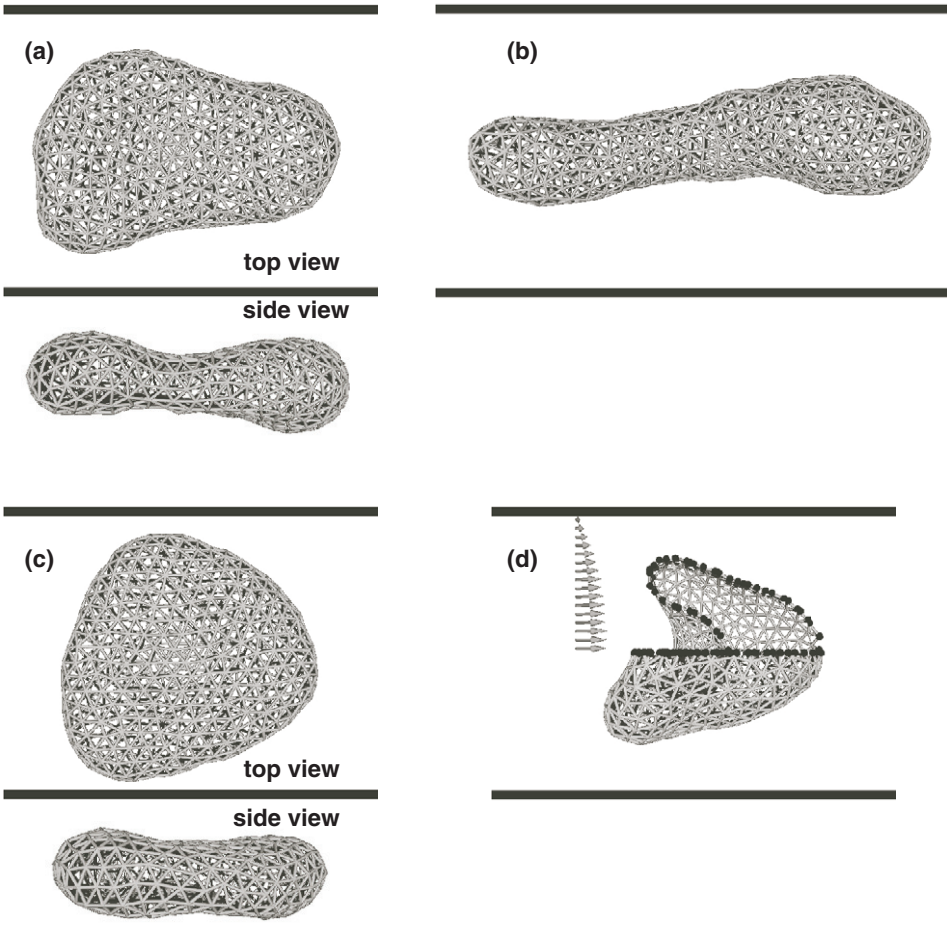

Figure 3. Snapshots of vesicles in capillary flow. Fluid vesicles with (a) discoidal and (b) prolate shapes are shown at the mean fluid velocity $v_m \tau / R_{cap} = 0.75$ and 2.0, respectively. Elastic vesicles (red blood cell model) with (c) discoidal and (d) parachute shapes are shown for $v_m \tau / R_{cap} = 0.71$ and 4.0, respectively. The arrows in (d) represent the velocity field of the solvent. The upper front quarter of the vesicle in (d) is removed to allow a look into the interior; the black circles indicate the lines where the membrane has been cut in this procedure. Thick lines indicate the walls of the cylindrical capillary. Walls are not shown in side views.

3.2. Capillary flow

Both fluid and elastic vesicles retain their discoidal shapes in slow capillary flows. We find that coaxial orientation with the capillary axis is unstable in slow flows. Instead, the vesicles align the longest axis of the moment-of-inertia tensor with the flow direction; see figures 3(a) and (c). The discoidal shape is elongated in the flow direction and its front–rear symmetry is broken, but the biconcave dimples and the mirror symmetry with respect to the plane determined by the two eigenvectors of the moment-of-inertia tensor with the largest eigenvalues are retained.

At larger mean fluid velocity $v_m \tau / R_{cap} > 1.0$, the fluid vesicle transits into a prolate ellipsoidal shape (figure 3(b)). On the other hand, the elastic vesicle transits into a parachute shape at $v_m \tau / R_{cap} > 1.5$ (figure 3(d)), because the shear elasticity prevents large shear deformations. Both shape transitions reduce the flow resistance.

In most previous theoretical and numerical studies [2], axisymmetric shapes which are coaxial with the centre of the capillary were assumed and cylindrical coordinates were employed. Our results show that this assumption is justified only for high fluid velocity.

In capillary flows, an effective shear rate can be defined as $\dot{\gamma}_{\rm eff} = 2v_{\rm m}/R_{\rm cap}$, because the mean flow velocity $v_{\rm m}$ is half of the maximum velocity in Poiseuille flow. This implies an effective shear rate of $\dot{\gamma}_{\rm eff}\tau = 2.0$ at the shape transitions of fluid vesicles from discocyte to prolate. This value coincides with the shear-induced discocyte-to-prolate transition in simple shear flow. Thus, the elongation transition is induced by the same amount of shear force in both flow fields.

4. Conclusions

We have investigated shape transitions of vesicles in simple shear and capillary flows. The flow fields induce discocyte-to-prolate, prolate-to-discocyte, and discocyte-to-parachute transformations. Our model has the advantage that it can easily be adapted to a variety of other problems of vesicle dynamics in flow, like multi-component vesicles and interactions between vesicles or a vesicle and a capillary wall.

Acknowledgment

We acknowledges partial support of this work by the Deutsche Forschungsgemeinschaft through the priority program 'Nano- and Microfluidics'.

References

[1] Seifert U 1997 *Adv. Phys.* **46** 13
[2] Skalak R 1990 *Biorheology* **27** 277
[3] Pries A R, Secomb T W and Gaehtgens P 1996 *Cardiovasc. Res.* **32** 654
[4] Tsukada K, Sekizuka E, Oshio C and Minamitani H 2001 *Microvasc. Res.* **61** 231
[5] Keller S R and Skalak R 1982 *J. Fluid Mech.* **120** 27
[6] Noguchi H and Gompper G 2004 *Phys. Rev. Lett.* **93** 258102
[7] Noguchi H and Gompper G 2005 *Phys. Rev.* E **72** 011901
[8] Noguchi H and Gompper G 2005 *Proc. Natl Acad. Sci. USA* **102** 14159
[9] Malevanets A and Kapral R 1999 *J. Chem. Phys.* **110** 8605
[10] Lamura A, Gompper G, Ihle T and Kroll D M 2001 *Europhys. Lett.* **56** 319
[11] Ripoll M, Mussawisade K, Winkler R G and Gompper G 2004 *Europhys. Lett.* **68** 106
[12] Gompper G and Kroll D M 1997 *J. Phys.: Condens. Matter* **9** 8795
[13] Gompper G and Kroll D M 2004 Triangulated-surface models of fluctuating membranes *Statistical Mechanics of Membranes and Surfaces* ed D R Nelson, T Piran and S Weinberg (Singapore: World Scientific)